Advances in Machinery, Materials Science and Engineering Application IX
M. Chen et al. (Eds.)

doi:10.3233/ATDE230539

Simulation of Car Body Deformation in Electrophoresis Process Based on Fluid-Structure Interaction Method

Baojun YU [a,1], Ding LI [a], Anyang XU [a], Yongjian HUANG [a] and Haidong LI [a]
[a] *China FAW Group Co., Ltd, Product Development Center, Changchun 130013 China*

Abstract. During the car body painting process, the car body is prone to deformation after being subjected to shock loads from electrophoresis fluid. The traditional solution is to adopt multiple rounds of test testing to verify the feasibility of the scheme and conduct an optimization plan attempt, undoubtedly requires a long period of time and a large amount of human and material resources. The multi-phase flow simulation method and overlapping mesh technology are used to simulate car body electrophoresis process, extract the electrophoresis shock load of the body, simulate the deformation of the body through the simulation method, and optimize the overall structure through the topology simulation method to reduce the deformation during the electrophoresis process. The simulation method is in good agreement with the test results, and can be used to simulate, predict and optimize the deformation of car body structure during the electrophoresis process in the product design and development stage.

Keywords. Electrophoretic car body deformation, fluid-structure interaction, multiphase flow, overset

1. Introduction

Coating process is one of the four major processes in automobile production, which is a process of drying and forming film after covering the surface of the body-in-white. The automobile coating line is mainly composed of electrophoresis line, sealing bottom coating line, intermediate coating line, surface coating line, finishing line and drying system. The electrophoresis line is made up of pretreatment, electric swimming pool, post-cleaning and other processes. In the process of the body-in-white passing through the electric pool at room temperature, the body-in-white is easy to deformed after being impacted by the electrophoretic fluid.

At present, the research of electrophoresis simulation at home and abroad are mainly focused on the numerical simulation of film quality. For example, ESS proposed a finite difference method to accurately and effectively simulate the industrial EPD coating process [1]. Dominik Bartuschat of the University of Nuremberg introduced a numerical coupling algorithm for the simulation of microfluidic electrophoresis membranes [2]. Karlsruhe Institute of Technology utilized a simulation mean to prove that the segmented electrode can effectively reduce the amount of

[1] Baojun YU, Corresponding author, China FAW Group Co., Ltd, Product Development Center, Changchun 130013 China; E-mail: demon98319@163.com

coating material under different potential differences [3]. SGMW simulated the electrophoretic film thickness of the body-in-white by CAE [4].

At present, the quality problems caused by body deformation during electrophoresis are solved mainly by using tests for verification and optimization. Song Xinduan of FAW-Volkswagen proposed that CMT welding can effectively reduce the electrophoretic deformation of the boot and reduce the matching defect rate of the rear body [5]. Zou Fengxiang of SGMW found that the deformation of the electrophoretic process can be reduced by optimizing the lock pin support point of the hood [6]. Yang Yunfeng of Zhengzhou Nissan optimized the fixed tooling by means of experiments, and solved the problem of electrophoretic deformation of the boot [7]. Although these methods can solve the problem of body deformation in the electrophoresis process, it requires multiple rounds of test and sample production, with long cycle and high cost.

In this paper, the electrophoretic process of the body-in-white is simulated by means of the fluid simulation software, get the impact load of the electrophoretic liquid on the body-in-white, the load is mapped to the solid model through unidirectional coupling, and the deformation of the body-in-white is calculated and compared with the test results, adjust the structure by using the structural optimization simulation to reduce sheet metal deformation. The technical route is shown in figure 1.

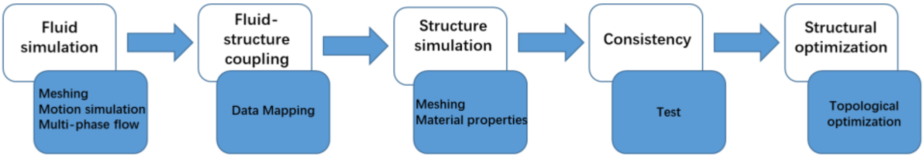

Figure 1. Technical route.

2. Fluid Simulation

In the process of electrophoresis, the body-in-white is subjected to the impact load of the electrophoretic fluid while moving in the electrophoretic fluid. In this paper, the fluid simulation is carried out by the STAR-CCM+. In order to obtain the impact load on the body-in-white, it is necessary to mesh the body-in-white and accessories, then use the overlapping mesh technology to simulate the body motion, and finally carry on the multiphase flow simulation.

2.1. Meshing

The modeling of body-in-white and fixture adopts the strategy of surface warper and local refinement. After adjusting the relative position, import the body-in-white and fixture model into Star-CCM+ for surface meshing. The parameters of surface wrapper and local refinement are shown in table 1 and table 2.

Table 1. Mesh Settings of Surface Wrapper.

	Surface wrapper	Local refinement (Closure)
Basic size	0.1m	-
Target size	0.016m	0.008m
Minimum size	0.016m	0.004m

Table 2. Mesh Settings of Mesh Reconstruction.

	Mesh reconstruction	Local refinement (Closure)
Basic size	0.1m	-
Target size	0.016m	0.004m
Minimum size	0.016m	0.002m

2.2. Motion Simulation

The computational mesh in fluid simulation analysis is the watershed itself, in order to keep the mesh fixed, in conventional simulation relative motion is often used. However, the movement of the body-in-white in the electrophoresis process is complex, so the above methods can not be used. Therefore, it is necessary to solve the two problems of complex motion trajectory and moving mesh.

2.2.1. Complex Motion Trajectory

As shown in figure 2, in the process of body electrophoresis, the body-in-white is locked by a fixed point and a sliding lever, which is connected to the lower end of the pendulum bar through two rotating mechanisms, the fixed distance between the upper and lower positioning points is h, h=3.25 m, and the upper end of the pendulum rod is driven by a transmission mechanism, moving uniformly along the track at a tangential speed of 2.97m/min with a total duration of 800s.

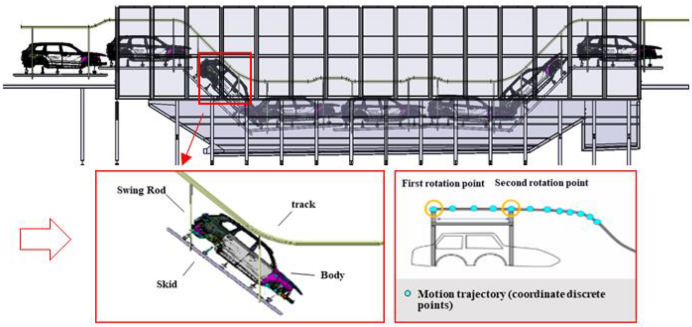

Figure 2. Electrophoretic motion process of body-in-white.

Motion simulation is performed by defining the rotation superimposed by constrained motion tracks in Star-CCM+. The track line of the guide rail is made as the discrete point of XYZ coordinates, in which the first rotation point is selected as the starting point of the track line, and the velocity is defined as 2.97m/min. The second rotation point is obtained by the first rotation point X to translate h distance, which is defined as a constrained rotation, then the body-in-white will move along the trajectory at the speed of 2.97m/min.

2.2.2. Overset

Dynamic mesh technology is generally used in fluid simulation to solve the problem of solid boundary motion, however this method takes a long time to calculate and has poor convergence. In this paper, overlapping mesh technology is used to discretize the electric pool and surrounding space into a background mesh. In the background mesh, the body movement area is discretized into a sub-region to save the simulation time.

The computing domain consist of the global computing domain and the local computing domain. The global computing domain composed of the electrophoresis tank, workshop, entrance, exit and entrance extension. The local computing domain includes the body in white and the surrounding fluid region , surrounded by a cuboid area of appropriate size (700 mm from the front end of the boundary to the front of the body-in-white, 900 mm from the rear of the body-in-white, 500 mm from the upper part of the body-in-white, 400 mm from the lower part of the accessories, and 500 mm from the left and right sides of the body-in-white). The surface of the box is set as an overlapping mesh interface as shown in figure 3.

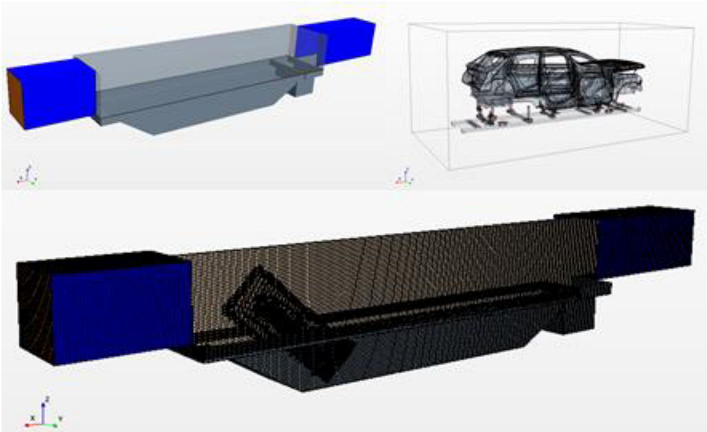

Figure 3. Overset of electrophoresis process.

2.3. Multiphase Flow Simulation

Considering the electrophoretic process of the body-in-white is affected by both the gas phase (air) and the liquid phase (electrophoretic fluid), in addition, the flow characteristics of the electrophoresis solution conform to the free level flow in the layered flow as a whole, so the fluid volume (VOF) multiphase model of Euler multiphase flow is used for simulation.
In VOF model, the distribution of phase and the position of interface are described by volume fraction, and the volume fraction of phase i is defined as formula (1).

$$\alpha_i = \frac{V_i}{V} \tag{1}$$

Where V_i is the volume of phase i in the specified mesh, and V is the volume of the specified mesh. The sum of the volume fractions of all phases is 1, $\sum_{i=1}^{N} \alpha_i = 1$, N is the total number of phases.

Based on the volume fraction, the distribution of phases in the fluid can be distinguished: $\alpha_i = 0$ indicates that there is no i phase in the mesh, and $\alpha_i = 1$ means that all phases in the mesh are phase i. $0 < \alpha_i < 1$ indicates that the mesh contains the interface of two phases.

In the mesh containing the intersecting interface, the material property is determined by the properties of the constituent phase. At the same intersecting interface, the fluid is a mixture, the multiphase flow density is equation (2), the kinetic viscosity is equation (3), and the specific heat is equation (4).

$$\rho = \sum_i \rho_i \alpha_i \tag{2}$$

$$\mu = \sum_i \mu_i \alpha_i \tag{3}$$

$$C_p = \sum_i \frac{(C_p)_i \rho_i}{\rho} \alpha_i \tag{4}$$

In the formula, ρ_i, $\mu_i$and $\left(C_p\right)_i$ are the density, kinetic viscosity and specific heat of phase i, respectively.

The phase distribution is driven by the mass conservation equation of equation (5)

$$\frac{\partial}{\partial t}\int_V \alpha_i dV + \oint_A \alpha_i \boldsymbol{v} \cdot d\boldsymbol{a} = \int_V \left(S_{\alpha_i} - \frac{\alpha_i}{\rho_i}\frac{D\rho_I}{Dt}\right) dV - \int_V \frac{1}{\rho_i}\nabla \cdot (\alpha_i \rho_i \boldsymbol{v_d}, i)d \tag{5}$$

In the formula, a is the area vector, V is the mixing (mass average) velocity, $v_{d,i}$ is the diffusion velocity, S_{α_i} is the self-defined source term of phase i, and $D\rho_i/Dt$ is the particle derivative of phase density ρ_i.

The Euler multiphase flow is selected in the Star-CCM+ physical model, and the material properties of the two phases are defined as electrophoretic liquid and air respectively. The initial phase composition is defined by the field function, and the definition function is shown in table 3.

Table 3. Multiphase flow function settings.

Function name	Contents
Electrophoretic solution	($${Position}[2]<-0.226384&&$${Position}[0]>-27.389117)?1:0
air	1-${Paint}

2.4. Solution Results

The impact load on the body-in-white varies from Water inflow to outflow. Figure 4 shows the pressure contours of the body-in-white and closure in these stages.

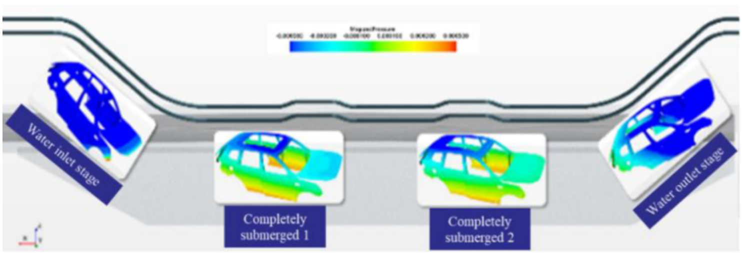

Figure 4. Pressure contours.

According to the analysis results, it is found that the pressure is well-distributed when the hood entering the water and immerged, while the hood leaving the water, there is an obvious pressure concentration at the front. According to the distribution of the flow field, it is caused by the negative pressure generated by the inner and outer plates when the electrophoresis fluid outlet the front chamber of the engine hood, as shown in figure 5.

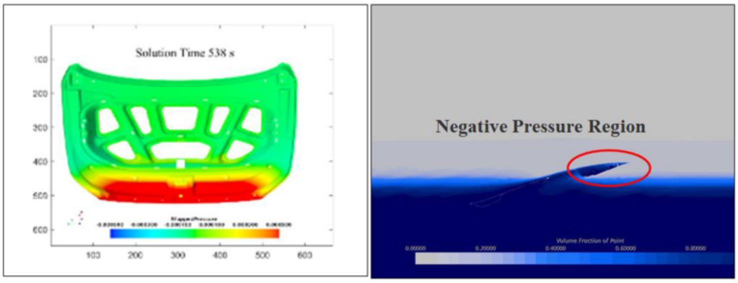

Figure 5. Pressure contour and flow field profile at water-exit time.

3. Fluid-structure Coupling

The relative relationship between the fluid boundary, the solid boundary and the normal direction of the shell element in the mesh mapping is shown in figure 6. The fluid pressure is always perpendicular to the solid wall pointing inside the solid, the pressure direction on the SPOS surface of the solid shell element is opposite to the normal direction of the shell element, and the pressure direction on the SNEG surface is the same as the normal direction of the shell element. The resultant forces on the inner and outer surfaces of the solid model are applied on the structure simulation model shell element. The normal direction of the shell element is the resultant force direction defined in the solid model.

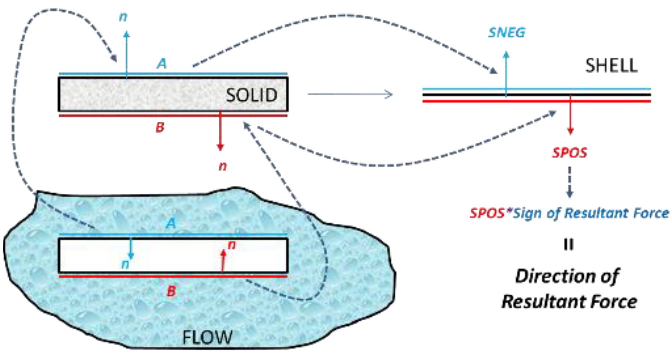

Figure 6. Normal relative relationship of model boundary in mesh mapping.

The commonly used mapping algorithms of fluid-solid coupling include Nearest Neighbor Interpolation (proximity interpolation), Least Squares Interpolation (least square interpolation), Exact Imprinting Interpolation (accurate imprinting interpolation) and Approximate Imprinting Interpolation (approximate imprinting interpolation).

In this paper, taking the engine cover pressure load at the water-exit time as the load, the CPU time, calculation memory and result consistency of the four methods are compared, in which the consistency is calculated according to formula (6).

$$\emptyset = 1 - \frac{\sum_{1}^{100}\left|\frac{P_{li}-P_{si}}{P_{li}}\right|}{100} \tag{6}$$

In the formula, P_{li} is the initial pressure of a certain point, P_{si} is the mapped pressure of a certain point, and 10×10 sampling points are selected in the normal projection direction of the outer plate of the engine hood.

The comparison results show that proximity interpolation is the algorithm with the highest efficiency but the lowest accuracy; the least square interpolation algorithm has moderate computational efficiency and accuracy; the accurate imprinting interpolation algorithm has the highest accuracy and the lowest efficiency; the computational efficiency of approximate imprint interpolation is similar to that of least square interpolation. However, the algorithm is globally conserved, but locally it is not strictly conserved. According to the comparison results, this paper uses the least square difference method with high accuracy and efficiency to carry out load mapping, as shown in table 4.

Table 4. Statistics of interpolation algorithms.

Interpolation algorithm	CPU time/s	Compute memory / MB	Mapping result consistency
Least squares	2.76	1632.75	92.58%
Precise Imprint	71.44	1565.30	96.85%
Approximate Imprint	4.26	1566.15	88.32%
Neighborhood	0.53	1520.13	75.35%

4. Structure Simulation

In this paper, the solid mesh of the engine hood is built by the software Abaqus, the mapped pressure load is loaded, and the deformation of the engine hood is obtained by implicit dynamic simulation, which is compared with test results.

4.1. Meshing

The solid mesh is discretized by full integral shell element mesh, the basic mesh size is 5mm, and the number of meshes is 3 million. Because the engine hood flanging edge deformation is mainly considered in the electrophoresis process, the engine hood outer plate flanging and inner plate interlayer need to be coupled by mesh imprint and adhesive solid element nodes to ensure the calculation accuracy of flanging edge deformation. The damping glue adopts full integral solid element to divide the mesh, and adopts common node coupling with the inner and outer plates to ensure the accuracy of pressure transmission, as shown in figure 7.

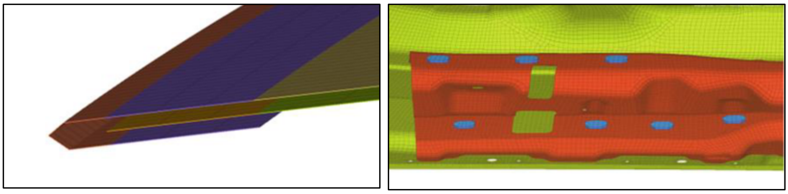

Figure 7. Solid mesh refinement.

The engine hood material is modeled by an elastic-plastic constitutive model, and the material card is fitted according to the real stress-strain curve converted from the static tensile test of GB/T 228.1-2010 material specimens. The material parameters are shown in table 5.

Table 5. Material parameters of engine hood.

parts	Elastic modulus/GPa	yield strength/MPa	tensile strength/MPa	Elongation/%
Outer plate	224.26	138.18	286.68	54.63
Inner plate	201.61	152.74	294.23	48.66
Reinforcing plate	206.35	223.11	335.63	45.12

4.2. Calculation Result

The body surface fluid pressure load is a time-varying pressure load that is loaded by a distributed force load as shown in figure 8, the front of the engine hood has the largest deformation at the moment of water-exit and the maximum deformation position occurs at the midpoint of the leading edge of the bonnet.

Selecting the middle position point of the front edge of the engine hood can obtain its z-direction deformation curve with time. Under the load of fluid pressure the maximum deformation occured at 538s, when the engine hood is in the water-exit stage and deformed 0.302mm.

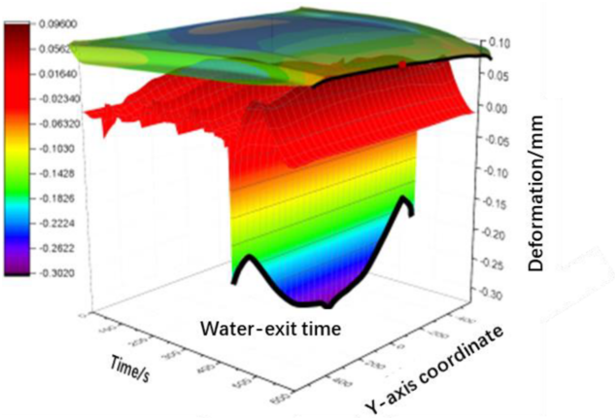

Figure 8. Deformation contours of engine hood front during electrophoresis process.

5. Consistency Comparison

The designed measuring tool is fixed on the electrophoretic supporting accessories of the engine hood, and the deformation of the front edge of the cover is evaluated by measuring the gap between the electrophoretic test tools and the electrophoretic aids before and after electrophoresis. A measuring point with equal distance from y to 50 mm is set at the leading edge of the engine hood, and the results are measured before and after electrophoresis. The results are shown in figure 9.

y/100	-3		-2.5		-2		-1.5		-1		-0.5		0	
process	Before electrophoresis	After electrophoresis	Before electrophoresis	After electrophoresis	Before electrophoresis	After electrophoresis	Before electrophoresis	After electrophoresis	Before electrophoresis	After electrophoresis	Before electrophoresis	After electrophoresis	Before electrophoresis	After electrophoresis
1	13.25	13.21	14.72	14.7	15.72	15.71	16.63	16.5	17.25	17.08	17.82	17.45	18.35	18.02
2	13.22	13.2	14.67	14.71	15.68	15.74	16.59	16.47	17.26	17.05	17.78	17.53	18.34	18
3	13.25	13.23	14.74	14.75	15.78	15.79	16.62	16.51	17.25	17.13	17.83	17.51	18.32	17.98
4	13.24	13.24	14.74	14.75	15.62	15.8	16.58	16.46	17.18	17.05	17.81	17.51	18.32	17.98
5	13.26	13.26	14.77	14.74	15.74	15.75	16.67	16.49	17.24	17.11	17.81	17.51	18.37	18
6	13.26	13.29	14.76	14.73	15.7	15.76	16.57	16.48	17.18	17.11	17.84	17.48	18.4	17.96
7	13.21	13.24	14.79	14.76	15.74	15.75	16.6	16.44	17.26	17.12	17.8	17.53	18.38	17.95

y/100	0.5		1		1.5		2		2.5		3	
process	Before electrophoresis	After electrophoresis	Before electrophoresis	After electrophoresis	Before electrophoresis	After electrophoresis	Before electrophoresis	After electrophoresis	Before electrophoresis	After electrophoresis	Before electrophoresis	After electrophoresis
1	18.15	17.84	18	17.72	17.32	17.25	16.35	16.34	14.92	15.04	12.88	13.47
2	18.15	17.83	18.02	17.71	17.29	17.19	16.39	16.33	14.89	15.05	12.9	13.45
3	18.2	17.82	17.99	17.72	17.32	17.22	16.39	16.32	14.96	15.06	12.87	13.47
4	18.15	17.84	17.98	17.67	17.39	17.21	16.38	16.29	14.95	15.07	12.95	13.44
5	18.22	17.82	18	17.71	17.32	17.21	16.39	16.31	14.89	15.11	12.85	13.48
6	18.18	17.81	17.99	17.71	17.28	17.19	16.36	16.26	14.96	15.05	12.91	13.48
7	18.18	17.83	17.98	17.67	17.32	17.2	16.4	16.32	14.91	15.1	12.95	13.45

Figure 9. Measuring method and data of cover deformation in electrophoresis process.

The data of all measuring points are analyzed, and the measurement errors are calculated. The average measurement error is about 0.08 mm, and the minimum and maximum errors are 0.056 mm and 0.134 mm. By checking the T distribution confidence interval table, 85% confidence interval is used to evaluate the measurement results to compare the effective measurement results with the simulation results, the average accuracy of simulation and test consistency is 86%, and the middle consistency of the front of the engine hood is 81.6%. The results are shown in figure 10.

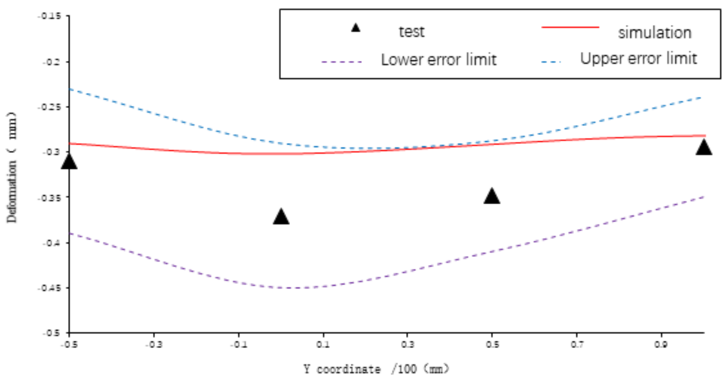

Figure 10. Consistency comparison results.

6. Structure Optimization

Using topology optimization analysis, the maximum displacement of the midpoint of the front edge of the engine hood is used as the constraint to find out the bearing path of the edge of the engine cover, and add Cold Metal Transfer (CMT) to the key nodes in the path to resist the leading edge deformation, as shown in figure 11.

Figure 11. Results of topology optimization.

Add one-sided welding to re-simulate, and the maximum deformation of the midpoint of the hood front was reduced by 0.15mm, as shown in figure 12.

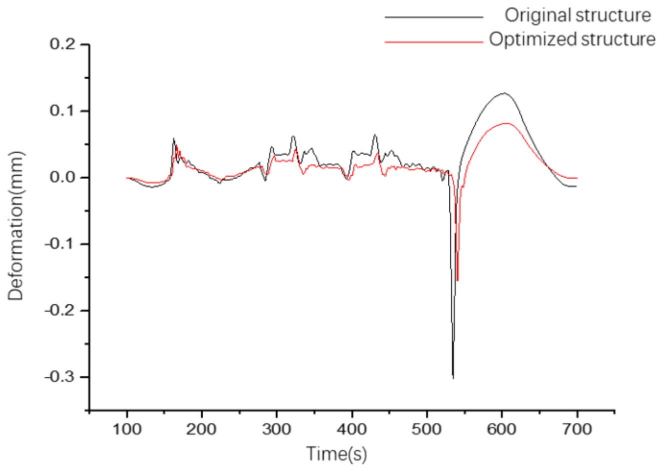

Figure 12. Comparison of engine hood deformation before and after optimization.

7. Concluding Remarks

In this paper, the fluid simulation method is used to simulate the electrophoresis process of the car body, the pressure load of the electrophoresis fluid subjected to the car body is obtained, the load is coupled to the solid model and simulated, and the calculation results are 81.6% consistent with the test results, and the simulation accuracy is high. The significance of this paper is as follows:

For the first time in China, fluid-structure interaction simulation technology is used to solve the deformation problem of body structure in the electrophoresis process, so as to advance the body structure deformation problem of the electrophoresis process to the product design stage, improve the original product development process that was only solved by experiment in the pre-batch stage, shorten the development cycle, and save the costs.

References

[1] Kevin V. Modeling and simulation of electrophoretic deposition coatings. Journal of Computational Science. ESS Engineering Software Steyr GmbH. 2020. 10. 1016/j. jocs. 2020.1010.
[2] Dominik B. A scalable multiphysics algorithm for massively parallel direct numerical simulations of electrop horetic motion. Journal of Computational Science. Fried rich-Alexander Universität Erlangen-Nürnberg. 2018. 10.1016/j. jocs.2018.05.011.
[3] Florian K, Hermann N. Efficient numerical simulation and optimiz ation in electrophoretic deposition processes. Journal of the European Ceramic Society. Karlsruhe Institute of Technology. 2015. 10.1016/j.jeurcera msoc.2015.02.031.
[4] Liu QQ, Yuan JB, Wei CZ. Application of electrophoretic simulation technology in the development of hood. Modern Finishing. 2018: 67-69.
[5] Song XD, Mu CY. Research of CMT welding technology in preventing electrophoresis distortion of automobile rear cover. Modern Manufacturing Technology and Equipment. 2020; (9):25-26.
[6] Zou FX, Zhou MH, Jiang LL. Improvement of coating process causing deformation of automobile hair cover. Chuang Xin Ke Ji. 2013; (10):73-74.
[7] Yang YF, Hou LL, pan LJ. Causes and solutions of deformation of trunk door after coating of pickup truck. The 15th Henan Automotive Engineering Science and Technology Symposium. 2018: 260-261.